

A Nonacoordinated Bridging Selenide in a Tricapped Trigonal Prismatic Geometry Identified in Undecanuclear Copper Clusters: Syntheses, Structures, and DFT Calculations

C. W. Liu,^{*,†} Chiu-Mine Hung,[†] Bidyut Kumar Santra,[†] Yi-Hua Chu,[†] Ju-Chun Wang,[‡] and Zhenyang Lin^{*,§}

Department of Chemistry, Chung Yuan Christian University, Chung-Li, Taiwan 320, Department of Chemistry, Soochow University, Taipei, Taiwan 111, and Department of Chemistry, The Hong Kong University of Science & Technology, Clear Water Bay, Kowloon, Hong Kong

Received March 29, 2004

Undecanuclear copper clusters, $[\text{Cu}_{11}(\mu_9\text{-Se})(\mu_3\text{-Br})_3\{\text{Se}_2\text{P}(\text{OR})_2\}_6]$ ($\text{R} = \text{Et}, \text{Pr}, \text{}^i\text{Pr}$) (**1a–c**), were isolated along with closed-shell ion-centered cubes, $[\text{Cu}_8(\mu_8\text{-Br})\{\text{Se}_2\text{P}(\text{OR})_2\}_6]$ (PF_6) (**2a–c**) and $[\text{Cu}_8(\mu_8\text{-Se})\{\text{Se}_2\text{P}(\text{OR})_2\}_6]$ (**3a–c**), from the reaction of $[\text{Cu}(\text{CH}_3\text{CN})_4](\text{PF}_6)$, $\text{NH}_4[\text{Se}_2\text{P}(\text{OR})_2]$, and Bu_4NBr in a molar ratio of 2:3:2 in CH_2Br_2 . The molecular formulations of these clusters were confirmed by elemental analysis, positive FAB mass spectrometry, and multinuclear NMR (^1H , ^{31}P , and ^{77}Se). ^{77}Se NMR spectra of Cu_{11} clusters (**1a–c**) are of special interest as two inequivalent selenium nuclei of the diselenophosphate (dsep) ligand exhibit different scalar coupling patterns with the adjacent phosphorus nuclei. X-ray analysis of **1c** reveals a Cu_{11}Se core stabilized by three bromide and six dsep ligands. The central core adopts the geometry of a 3,3,4,4,4-pentacapped trigonal prism with a selenium atom in the center. The coordination geometry for the nonacoordinated selenium atom is tricapped trigonal prismatic. The X-ray structure **2a** or **2c** consists of a cationic cluster in which eight copper ions are linked by six diselenophosphate ligands with a central $\mu_8\text{-Br}$ ion. The shape of the molecule is a bromide-centered distorted Cu_8 cube. Each diselenophosphate ligand occupies square faces of the cube and adopts a tetrametallic tetraconnective coordination pattern. Each copper atom of the cube is coordinated by three selenium atoms with a strong interaction with the central bromide ion. Molecular orbital calculations at the B3LYP level of the density functional theory have been carried out to study the $\text{Cu}-\mu_9\text{-Se}$ interactions for clusters $[\text{Cu}_{11}(\mu_9\text{-Se})(\mu_3\text{-X})_3\{\text{Se}_2\text{P}(\text{OR})_2\}_6]$ ($\text{X} = \text{Br}, \text{I}$). Calculations show that the formal bond order of each $\text{Cu}-\mu_9\text{-Se}$ bond is slightly smaller than half of those calculated for the terminal $\text{Cu}-\mu_2\text{-Se}$ bonds.

Introduction

The hypercoordination of main group elements has attracted much attention because they are related to anionic binding and recognition¹ and anion template effects² and involved in supramolecular chemistry.³ The halide ions are studied to the greatest extent due to their variable coordination modes, and the coordination polyhedra for the halides

are planar,⁴ tetrahedral,⁵ octahedral,⁶ and cubic.⁷ Molecular cubic clusters encapsulating main group elements are not only rare but also particularly interesting in view of their unusual bonding characteristics.⁸ Several cubic clusters encapsulating S^{2-} , Cl^- , and Br^- are known for the dithiophosphate ligand.⁹ The corresponding selenium-containing compounds have received attention only in recent years from

* To whom correspondence should be addressed at the Chung Yuan Christian University. E-mail: chenwei@cycu.edu.tw (C.W.L). Fax: (+886) 3-265-3399.

[†] Chung Yuan Christian University.

[‡] Soochow University.

[§] Hong Kong University of Science & Technology.

(1) (a) Beer, P. D.; Gale, P. A. *Angew. Chem., Int. Ed.* **2001**, *40*, 486. (b) Pratt, M. D.; Beer, P. D. *Polyhedron* **2003**, *22*, 649.

(2) (a) Sessler, J. L.; Sansom, P. I.; Andrievsky, A.; Gale, P. A.; Lynch, V. *Angew. Chem., Int. Ed. Engl.* **1996**, *35*, 2782. (b) Zheng, Z.; Knobler, C. B.; Hawthorne, M. F. *J. Am. Chem. Soc.* **1995**, *117*, 5105. (c) Yang, X.; Knobler, C. B.; Zheng, Z.; Hawthorne, M. F. *J. Am. Chem. Soc.* **1994**, *116*, 7142. (d) Salta, J.; Chen, Q.; Chang, Y.; Zubieta, J. *Angew. Chem., Int. Ed. Engl.* **1994**, *33*, 757. (e) Sessler, J. L.; Mody, T. D.; Lynch, V. *J. Am. Chem. Soc.* **1993**, *115*, 3346. (f) Müller, A.; Rohlffing, R.; Krickemeyer, E.; Penk, M.; Bögge, H. *Angew. Chem., Int. Ed. Engl.* **1993**, *32*, 909.

our research group. With the diselenophosphate ligands, we reported the first selenide-centered Cu_8^{I} cubes, $[\text{Cu}_8(\mu_8\text{-Se})\{\text{Se}_2\text{P}(\text{O}^i\text{Pr})_2\}_6]$,¹⁰ and subsequently a cocrystallized product of $[\text{Ag}_8(\mu_8\text{-Se})\{\text{Se}_2\text{P}(\text{O}^i\text{Pr})_2\}_6]$ and $[\text{Ag}_6\{\text{Se}_2\text{P}(\text{O}^i\text{Pr})_2\}_6]$.¹¹ To extend our research efforts in main-group element encapsulated cubic clusters synthesis, we turned our attention to the bromide ion and uncovered, besides a selenide-centered Cu_8^{I} cube, a bromide-centered Cu_8^{I} cube and a novel noncoordinated selenide in a tricapped trigonal prismatic geometry in Cu_{11} cluster. Tricapped trigonal prism is the most commonly observed coordination geometry for a central atom surrounded by nine outer ligand atoms. This geometry has been observed in lanthanide complexes,¹² $[\text{ReH}_9]^{2-}$, and its derivatives.¹³ For a main-group element tricapped trigonal prismatic geometry has never been observed previously,

- (3) (a) *Supramolecular Chemistry of Anions*; Bianchi, A., Bowman-James, K., García-España, E., Eds.; Wiley-VCH: New York, 1997. (b) Vilar, R.; Migos, D. M. P.; White, A. J. P.; Williams, D. J. *Angew. Chem., Int. Ed.* **1998**, *37*, 1258. (c) Gale, P. A. *Coord. Chem. Rev.* **2000**, *199*, 181. (d) Coles, S. J.; Frey, J. G.; Gale, P. A.; Hursthouse, M. B.; Light, M. E.; Navakhun, K.; Thomas, G. L. *Chem. Commun.* **2003**, 568. (e) Du, M.; Bu, X.-H.; Huang, Z.; Chen, S.-T.; Guo, Y.-M. *Inorg. Chem.* **2003**, *42*, 552.
- (4) (a) Wang, R.; Selby, H. D.; Liu, H.; Carducci, M. D.; Jin, T.; Zhang, Z.; Anthis, J. W.; Staples, R. J. *Inorg. Chem.* **2002**, *41*, 278. (b) Wang, R.; Jin, T.; Zhang, Z.; Staples, R. J. *Angew. Chem., Int. Ed.* **1999**, *38*, 1813. (c) Yang, X.; Knobler, C. B.; Hawthorne, M. F. *Angew. Chem., Int. Ed. Engl.* **1991**, *11*, 1507.
- (5) (a) Gonzalez-Duarte, P.; Clegg, W.; Casals, I.; Sola, J.; Rius, J. J. *Am. Chem. Soc.* **1998**, *120*, 1260. (b) Dance, I. G. *Aust. J. Chem.* **1985**, *38*, 1391.
- (6) (a) Lee, H.; Knobler, C. B.; Hawthorne, M. F. *J. Am. Chem. Soc.* **2001**, *123*, 3148. (b) Krautscheid, H.; Lode, C.; Vielsack, F.; Vollmer, H. J. *Chem. Soc., Dalton Trans.* **2001**, 1099. (c) Lee, H.; Knobler, C. B.; Hawthorne, M. F. *Angew. Chem., Int. Ed.* **2000**, *39*, 776. (d) Wang, Q.-M.; Mak, T. C. W. *Chem. Commun.* **2000**, 1435.
- (7) (a) Burgi, H. B.; Gehr, H.; Strickler, P.; Winkler, F. K. *Helv. Chem. Acta* **1976**, *59*, 2558. (b) Dance, I. G.; Garbutt, R.; Craig, D. *Inorg. Chem.* **1987**, *26*, 3732. (c) Liu, C. W.; Hung, C.-M.; Haia, H.-C.; Liaw, B.-J.; Liou, L.-S.; Tsai, Y.-F.; Wang, J.-C. *Chem. Commun.* **2003**, 976.
- (8) (a) Garland, M. T.; Halet, J.-F.; Saillard, J.-Y. *Inorg. Chem.* **2001**, *40*, 3342. (b) Gautier, R.; Ogliaro, F.; Halet, J.-F.; Saillard, J.-Y.; Baerends, E. *Eur. J. Inorg. Chem.* **1999**, 1161. (c) Gautier, R.; Halet, J.-F.; Saillard, J.-Y. *Eur. J. Inorg. Chem.* **1999**, 673. (d) Zouchoune, B.; Ogliaro, F.; Halet, J.-F.; Saillard, J.-Y.; Eveland, J. R.; Whitmire, K. H. *Inorg. Chem.* **1998**, *37*, 865. (e) Furet, E.; Le Beuze, A.; Halet, J.-F.; Saillard, J.-Y. *J. Am. Chem. Soc.* **1995**, *117*, 4936. (f) Furet, E.; Le Beuze, A.; Halet, J.-F.; Saillard, J.-Y. *J. Am. Chem. Soc.* **1994**, *116*, 274. (g) Wheeler, R. A. *J. Am. Chem. Soc.* **1990**, *112*, 8737.
- (9) (a) Liu, C. W.; Stubbs, R. T.; Staples, R. J.; Fackler, J. P., Jr. *J. Am. Chem. Soc.* **1995**, *117*, 9778. (b) Fackler, J. P., Jr. *Inorg. Chem.* **2002**, *41*, 6959. (c) Fackler, J. P., Jr.; Staples, R. J.; Liu, C. W.; Stubbs, R. T.; Lopez, C.; Pitts, J. T. *Pure Appl. Chem.* **1998**, *70*, 839. (d) Huang, Z.-X.; Lu, S.-F.; Huang, J.-Q.; Wu, D.-M.; Huang, J.-L. *J. Struct. Chem.* **1991**, *10*, 213. (e) Wu, D.-M.; Huang, J.-Q.; Lin, Y.; Huang, J.-L. *Sci. Sin. Ser. B (Engl. Ed.)* **1988**, *31*, 800. (f) Matsumoto, K.; Tanaka, R.; Shimomura, R.; Nakao, Y. *Inorg. Chim. Acta* **2000**, *304*, 293.
- (10) Liu, C. W.; Chen, H.-C.; Wang, J.-C.; Keng, T.-C. *Chem. Commun.* **1998**, 1831.
- (11) Liu, C. W.; Shang, I.-J.; Wang, J.-C.; Keng, T.-J. *Chem. Commun.* **1999**, 995.
- (12) (a) White, J. P.; Deng, H.; Boyd, E. P.; Gallucci, J.; Shore, S. G. *Inorg. Chem.* **1994**, *33*, 1685. (b) Baggio, R.; Garland, M. T.; Perce, M. *Inorg. Chem.* **1997**, *36*, 950. (c) Martin, N.; Bunzli, J. C. G.; Mckee, V.; Piguat, C.; Hopfgartner, G. *Inorg. Chem.* **1998**, *37*, 577. (d) Mullica, D. F.; Farmer, J. M.; Kautz, J. A. *Inorg. Chem. Commun.* **1999**, *2*, 73. (e) Favas, M. C.; Kepert, D. L. *Prog. Inorg. Chem.* **1981**, *28*, 309.
- (13) (a) Abrahams, S. C.; Ginsberg, A. P.; Knox, K. *Inorg. Chem.* **1964**, *3*, 558. (b) Baudry, D.; Ephritikhine, M.; Felkin, H. *J. Organomet. Chem.* **1982**, *224*, 363. (c) Luo, X.-L.; Baudry, D.; Boydell, P.; Charpin, P.; Nierlich, M.; Ephritikhine, M.; Crabtree, R. H. *Inorg. Chem.* **1990**, *29*, 1511.

although a main-group element in the cavity of a mono-capped square antiprism is known in a couple of metal carbonyls.¹⁴ The isolated undecanuclear copper cluster is a remarkable example of possessing a 3,3,4,4,4-pentacapped trigonal prismatic copper framework. A preliminary account of our results has been communicated.¹⁵ Herein, we report the detailed syntheses and characterizations of undecanuclear copper clusters, $[\text{Cu}_{11}(\mu_9\text{-Se})(\mu_3\text{-Br})_3\{\text{Se}_2\text{P}(\text{OR})_2\}_6]$ (R = Et, Pr, ⁱPr) (**1a–c**), and bromide-centered Cu_8^{I} cubic clusters, $[\text{Cu}_8(\mu_8\text{-Br})\{\text{Se}_2\text{P}(\text{OR})_2\}_6](\text{PF}_6)$ (**2a–c**). In addition, the Cu– $\mu_9\text{-Se}$ interactions in clusters $[\text{Cu}_{11}(\mu_9\text{-Se})(\mu_3\text{-X})_3\{\text{Se}_2\text{P}(\text{OR})_2\}_6]$ (X = Br, I) have been studied by molecular orbital calculations at the B3LYP level of the density functional theory.

Experimental Section

Materials and Measurements. All chemicals were purchased from commercial sources and used as received. Commercial $\text{CH}_2\text{-Cl}_2$ and ROH were distilled from P_4O_{10} and Mg, respectively. Hexane and diethyl ether were distilled from Na/K. All the reactions were performed in oven-dried Schlenk glassware by using standard inert-atmosphere techniques. The starting copper(I) complex, $\text{Cu}(\text{CH}_3\text{CN})_4(\text{PF}_6)$,¹⁶ and the ligand, $\text{NH}_4\text{Se}_2\text{P}(\text{OR})_2$ (R = Et, Pr, ⁱPr),¹⁷ were prepared according to the literature methods. Silica gel 60 (0.063–0.20 mm) was used for column chromatography. The elemental analyses were done using a Perkin-Elmer 2400 CHN analyzer. NMR spectra were recorded on a Bruker AC-F200 and Advance-300 Fourier transform spectrometers. The $^31\text{P}\{^1\text{H}\}$ and $^{77}\text{Se}\{^1\text{H}\}$ NMR are referenced externally against 85% H_3PO_4 ($\delta = 0$) and PhSeSePh ($\delta = 463$), respectively. Positive FAB mass spectra were carried out on a VG 70-250S mass spectrometer with nitrobenzyl alcohol as the matrix.

Preparation of $[\text{Cu}_{11}(\mu_9\text{-Se})(\mu_3\text{-Br})_3\{\text{Se}_2\text{P}(\text{OR})_2\}_6]$ (R = Et, Pr, ⁱPr) (1a–c**) and $[\text{Cu}_8(\mu_8\text{-Br})\{\text{Se}_2\text{P}(\text{OR})_2\}_6](\text{PF}_6)$ (**2a–c**).** The compounds were prepared by following a general procedure with respective Et, Pr, and ⁱPr derivatives of the ligand. Dibromomethane (50 mL) was added to a Schlenk flask (100 mL) containing $\text{NH}_4\text{-}[\text{Se}_2\text{P}(\text{OEt})_2]$ (1.130 g, 3.80 mmol), and the solution was stirred for 0.5 h at 0 °C. Then Bu_4NBr (0.815 g, 2.53 mmol) and $[\text{Cu}(\text{CH}_3\text{CN})_4](\text{PF}_6)$ (0.942 g, 2.53 mmol) were added sequentially. The solution mixture was stirred for 4 h at 0 °C under a dinitrogen atmosphere where the solution color changed from colorless to yellow during the reaction period. After filtration, the yellow filtrate was evaporated to dryness under vacuum. Then it was extracted with hexane (100 mL) to afford a yellow solution and white precipitate. The white precipitate was washed with methanol, which yielded the pure compound $[\text{Cu}_8(\mu_8\text{-Br})\{\text{Se}_2\text{P}(\text{OEt})_2\}_6](\text{PF}_6)$ (**2a**) in 17% yield (0.130 g). Solvent was removed by rotary evaporation from the yellow hexane extract. Then, the residue was subjected to silica gel column chromatography using 4:3 ethyl acetate/*n*-hexane as the eluent, which yielded first a yellow band of $[\text{Cu}_8(\mu_8\text{-Se})\{\text{Se}_2\text{P}(\text{OEt})_2\}_6]$ (**3a**) (0.229 g, 32%) and then an orange band of $[\text{Cu}_{11}(\mu_9\text{-Se})(\mu_3\text{-Br})_3\{\text{Se}_2\text{P}(\text{OEt})_2\}_6]$ (**1a**) (0.290 g, 47%).

- (14) (a) Vidal, J. L.; Walker, W. E.; Pruett, R. L.; Schoening, R. C. *Inorg. Chem.* **1979**, *18*, 129. (b) Mackay, K. M.; Nicholson, B. K.; Robinson, W. T.; Sims, A. W. *J. Chem. Soc., Chem. Commun.* **1984**, 1276.
- (15) Liu, C. W.; Hung, C.-M.; Chen, H.-C.; Wang, J.-C.; Keng, T.-J.; Guo, K.-M. *Chem. Commun.* **2000**, 1897.
- (16) Kubas, G. J. *Inorg. Synth.* **1979**, *19*, 90.
- (17) (a) Kudchadker, M. V.; Zingaro, R. A.; Irgolic, K. J. *Can. J. Chem.* **1968**, *46*, 1415. (b) Liu, C. W.; Shang, I.-J.; Hung, C.-M.; Wang, J.-C.; Keng, T.-C. *J. Chem. Soc., Dalton Trans.* **2002**, 1974.

Table 1. Selected Crystallographic Data for [Cu₁₁(μ₉-Se)(μ₃-Br)₃{Se₂P(OⁱPr)₂}]₆ (**1c**), [Cu₈(μ₈-Br){Se₂P(OEt)₂}]₆(PF₆) (**2a**), and [Cu₈(μ₈-Br){Se₂P(OⁱPr)₂}]₆(PF₆) (**2c**)

	1c	2a·3/2H₂O	2c
formula	C ₃₆ H ₈₄ O ₁₂ P ₆ Se ₁₃ Br ₃ Cu ₁₁	C ₂₄ H ₆₃ F ₆ O _{13.5} P ₇ Se ₁₂ BrCu ₈	C ₃₆ H ₈₄ F ₆ O ₁₂ P ₇ Se ₁₂ BrCu ₈
fw	2860.00	2434.28	2575.57
space group	<i>P</i> $\bar{1}$	<i>R</i> 3 <i>c</i>	<i>C</i> 2/ <i>c</i>
<i>a</i> , Å	15.2820(8)	17.752(4)	24.345(5)
<i>b</i> , Å	15.5376(8)	17.752(4)	13.151(3)
<i>c</i> , Å	20.4796(11)	72.63(2)	24.991(5)
α, deg	93.011(1)	90	90
β, deg	106.941(1)	90	91.34(3)
γ, deg	108.216(1)	120	90
<i>V</i> , Å ³	4363.1(4)	19 823(8)	7999(3)
<i>Z</i>	2	12	4
ρ _{calcd} , g cm ⁻³	2.177	2.447	2.139
λ(Mo Kα), Å	0.710 73	0.710 73	0.710 73
μ, mm ⁻¹	9.568	9.97	8.241
<i>T</i> , K	298(2)	295(2)	293(2)
<i>R</i> 1 ^a	0.0639	0.0657	0.0502
w <i>R</i> 2 ^b	0.1397	0.1601	0.1096

$${}^a R_1 = \sum |F_o| - |F_c| / \sum |F_o|. \quad {}^b wR_2 = \{ \sum [w(F_o^2 - F_c^2)^2] / \sum [w(F_o^2)^2] \}^{1/2}.$$

The selenium-centered Cu₈ cube, [Cu₈(μ₈-Se){Se₂P(OR)₂}]₆, is known to form without the presence of halide ion.^{10,18}

Compound 1a. (Yield: ~47%, 0.290 g.) Anal. Calcd for C₂₄H₆₀-Cu₁₁O₁₂P₆Se₁₃Br₃: C, 10.71; H, 2.25. Found: C, 10.29; H, 2.10. FAB MS [*m/z* (*m/z*_{calcd})]: 2689.9 (2691.8), (M)⁺; 2610.7 (2611.9), (M - Br)⁺; 2413.2 (2412.8), (M - dsep)⁺. ¹H NMR (CDCl₃): δ 1.36 [t; 36H, OCH₂CH₃, *J*_{HH} = 7 Hz], 4.14 [m, 12H, OCH₂CH₃], 4.31 [m, 12H, OCH₂CH₃]. ³¹P{¹H} NMR (CDCl₃): δ 81.7 [s, 6P, P(OR)₂], *J*_{PSe} = 651, 675 Hz]. ⁷⁷Se{¹H} NMR (CDCl₃): δ -1220 [μ₉-Se], 44.4 (6Se, Se₂P(OR)₂), *J*_{SeP} = 651 Hz], -5.69 (6Se, Se₂P(OR)₂), *J*_{SeP} = 677) Hz].

Compound 1b. (Yield: ~43%, 0.283 g.) Anal. Calcd for C₃₆H₈₄-Cu₁₁O₁₂P₆Se₁₃Br₃·C₆H₁₄: C, 17.12; H, 3.35. Found: 17.98; H, 3.74. FAB MS [*m/z* (*m/z*_{calcd})]: 2858.8 (2860.1), (M)⁺; 2779.6 (2780.2), (M - Br)⁺; 2552.6 (2553.0), (M - dsep)⁺. ¹H NMR (CDCl₃): δ 0.94 (t; 18H, OCH₂CH₂CH₃, *J*_{HH} = 7 Hz), 0.95 (t; 18H, OCH₂-CH₂CH₃, *J*_{HH} = 7 Hz), 1.73 [m; 24H, OCH₂CH₂CH₃], 4.01 [m, 12H, OCH₂CH₂CH₃], 4.77 [m, 12H, OCH₂CH₂CH₃]. ³¹P{¹H} NMR (CDCl₃): δ 79.6 [s, 6P, P(OR)₂], *J*_{PSe} = 650, 675 Hz]. ⁷⁷Se{¹H} NMR (CDCl₃): δ -1193 [μ₉-Se], 70.0 (6Se, Se₂P(OR)₂), *J*_{SeP} = 651 Hz], 9.2 (6Se, Se₂P(OR)₂), *J*_{SeP} = 677) Hz].

Compound 1c. (Yield: ~46%, 0.302 g.) Anal. Calcd for C₃₆H₈₄-Cu₁₁O₁₂P₆Se₁₃Br₃·1/2C₆H₁₄: C, 16.13; H, 3.13. Found: C, 16.15; H, 3.25. FAB MS [*m/z* (*m/z*_{calcd})]: 2859.4 (2860.1), (M)⁺; 2779.3 (2780.2), (M - Br)⁺; 2552.1 (2553.0), (M - dsep)⁺. ¹H NMR (CDCl₃): δ 1.34 [d; 36H, OCH(CH₃)₂, *J*_{HH} = 6 Hz], 1.37 [d; 36H, OCH(CH₃)₂, *J*_{HH} = 6 Hz], 4.75 [m; 6H, OCH(CH₃)₂], 5.17 [m; 6H, OCH(CH₃)₂]. ³¹P{¹H} NMR (CDCl₃): δ 74.8 [s, 6P, P(OR)₂], *J*_{PSe} = 647, 668 Hz], -143.0 (septet, PF₆⁻, *J*_{PF} = 712). ⁷⁷Se{¹H} NMR (CDCl₃): δ -1201 [μ₉-Se], 61.72 [d, 6Se, Se₂P(OR)₂], *J*_{SeP} = 650 Hz], 0.10 [d, 6Se, Se₂P(OR)₂], *J*_{SeP} = 679 Hz].

Compound 2a. (Yield: ~17%, 0.13 g.) Anal. Calcd for C₂₄H₆₀-BrCu₈F₆O₁₂P₇Se₁₂: C, 11.97; H, 2.51. Found: C, 11.92; H, 2.32. FAB MS [*m/z* (*m/z*_{calcd})]: 2262.3 (2262.4), (M - PF₆)⁺. ¹H NMR (CDCl₃): δ 1.40 [t; 36H, OCH₂CH₃, *J*_{HH} = 7 Hz], 4.19 [m, 24H, OCH₂CH₃]. ³¹P{¹H} NMR (CDCl₃): δ 74.2 [s, 6P, P(OR)₂], *J*_{PSe} = 653 Hz], -143.0 (septet, PF₆⁻, *J*_{PF} = 712). ⁷⁷Se{¹H} NMR (CDCl₃): δ -23.2 [d, 12Se, Se₂P(OR)₂], *J*_{SeP} = 650 Hz].

Compound 2b. (Yield: ~13%, 0.106 g.) Anal. Calcd for C₃₆H₈₄-BrCu₈F₆O₁₂P₇Se₁₂: C, 16.79; H, 3.29. Found: 16.75; H, 3.04. FAB MS [*m/z* (*m/z*_{calcd})]: 2430.3 (2430.7), (M - PF₆)⁺. ¹H NMR (CDCl₃): δ 0.97 (t; 36H, OCH₂CH₂CH₃, *J*_{HH} = 7 Hz), 1.77 [m; 24H, OCH₂CH₂CH₃], 4.05 [m, 24H, OCH₂CH₂CH₃]. ³¹P{¹H} NMR

(CDCl₃) δ 74.7 [s, 6P, P(OR)₂], *J*_{PSe} = 652 Hz], -143.0 (septet, PF₆⁻, *J*_{PF} = 712). ⁷⁷Se{¹H} NMR (CDCl₃): δ -16.7 [d, 12Se, Se₂P(OR)₂], *J*_{SeP} = 650 Hz].

Compound 2c. (Yield: ~17%, 0.138 g.) Anal. Calcd for C₃₆H₈₄-BrCu₈F₆O₁₂P₇Se₁₂: C, 16.79; H, 3.29. Found: C, 16.75; H, 3.20. FAB MS [*m/z* (*m/z*_{calcd})]: 2430.5 (2430.7), (M - PF₆)⁺. ¹H NMR (CDCl₃): δ 1.41 [d; 72H, OCH(CH₃)₂, *J*_{HH} = 6 Hz], 4.81 [m; 12H, OCH(CH₃)₂]. ³¹P{¹H} NMR (CDCl₃): δ 68.2 [s, 6P, P(OR)₂], *J*_{PSe} = 648 Hz], -143.0 (septet, PF₆⁻, *J*_{PF} = 712). ⁷⁷Se{¹H} NMR (CDCl₃): δ -0.2 [d, 12Se, Se₂P(OR)₂], *J*_{SeP} = 651 Hz].

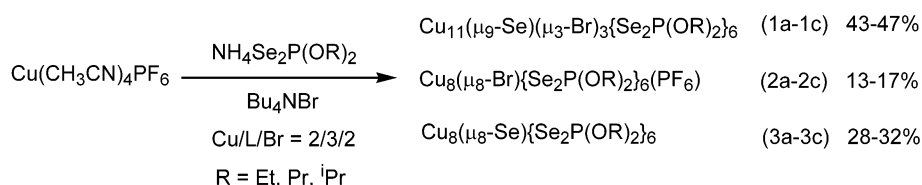
Safety Note. Selenium and its derivatives are toxic! These materials should be handled with great caution.

X-ray Crystallographic Procedures. The structures of [Cu₁₁(μ₉-Se)(μ₃-Br)₃{Se₂P(OⁱPr)₂}]₆ (**1c**), [Cu₈(μ₈-Br){Se₂P(OEt)₂}]₆(PF₆) (**2a**), and [Cu₈(μ₈-Br){Se₂P(OⁱPr)₂}]₆(PF₆) (**2c**) were obtained by the single-crystal X-ray diffraction technique. Crystals were mounted on the tips of glass fibers with epoxy resin. Data were collected on a Siemens SMART CCD (charged-coupled device) diffractometer for compounds **1c**. Cell parameters were retrieved with SMART software¹⁹ and refined with SAINT software²⁰ on all observed reflection (*I* > 10σ(*I*)). Data reduction was performed with SAINT, which corrects for Lorentz and polarization effects. For compounds **2a,c** data were collected at 293 K on a P4 diffractometer using graphite-monochromated Mo Kα radiation (λ = 0.710 73 Å) and were corrected for Lorentzian, polarization, and Ψ-scan absorption effects. The structures of **1c** and **2a,c** were solved by the use of direct methods, and refinement was performed by the least-squares methods on *F*² with the SHELXL-97 package,²¹ incorporated in SHELXTL/PC V5.10.²² Selected crystal data for the compounds (**1c**, **2a,c**) are summarized in Table 1.

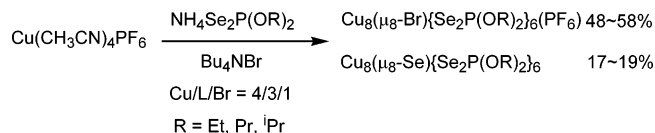
Compound 1c. Crystals suitable for X-ray diffraction were grown from CH₂Br₂ layered with hexane. A yellow crystal (0.40 × 0.38 × 0.25 mm) was mounted, and data were collected. A total

- (18) Liu, C. W.; Chen, H.-C.; Wang, J.-C.; Keng, T.-C. *Angew. Chem., Int. Ed.* **2001**, *40*, 2342.
- (19) SMART V4.043: Software for the CCD Detector System; Bruker Analytical X-ray Systems: Madison, WI, 1995.
- (20) SAINT V4.043: Software for the CCD Detector System; Bruker Analytical X-ray Systems: Madison, WI, 1995.
- (21) SHELXL-97: Sheldrick, G. M. *Program for the Refinement of Crystal Structure*; University of Göttingen: Göttingen, Germany, 1997.
- (22) SHELXL 5.10 (PC version): Program Library for Structure Solution and Molecular Graphics; Bruker Analytical X-ray Systems: Madison, WI, 1998.

Scheme 1



Scheme 2



of 20 983 reflections were collected, of which 14 482 were unique ($R_{\text{int}} = 0.0398$) and 11 404 were observed with $I > 2\sigma(I)$. H-atoms were added in the idealized positions. The final cycle of the full-matrix least-squares refinement was based on 11 404 observed reflections, 4 restraints, and 702 parameters and converged with unweighted and weighted agreement factors of $R1 = 0.0639$ and $wR2 = 0.1397$, respectively. The largest residual peak and hole are 1.148 and $-0.974 \text{ e}/\text{\AA}^3$.

Compound 2a·3/2H₂O. Crystals suitable for X-ray diffraction were grown from CH_2Br_2 layered with hexane. A colorless crystal ($0.40 \times 0.40 \times 0.30 \text{ mm}$) was mounted, and data were collected. A total of 8459 reflections were collected, of which 3888 were unique ($R_{\text{int}} = 0.0904$) and 2022 were observed with $I > 2\sigma(I)$. H-atoms were added in the idealized positions. The final cycle of the full-matrix least-squares refinement was based on 2022 observed reflections and 216 parameters and converged with unweighted and weighted agreement factors of $R1 = 0.0657$ and $wR2 = 0.1601$, respectively. The largest residual peak and hole are 1.221 and $-1.292 \text{ e}/\text{\AA}^3$.

Compound 2c. Crystals suitable for X-ray diffraction were grown from CH_2Br_2 layered with hexane. A colorless crystal ($0.50 \times 0.40 \times 0.20 \text{ mm}$) was mounted, and data were collected. A total of 11 231 reflections were collected, of which 6703 were unique ($R_{\text{int}} = 0.0356$) and 5589 were observed with $I > 2\sigma(I)$. H-atoms were added in the idealized positions. The final cycle of the full-matrix least-squares refinement was based on 5589 observed reflections and 382 parameters and converged with unweighted and weighted agreement factors of $R1 = 0.0502$ and $wR2 = 0.1096$, respectively. The largest residual peak and hole are 0.580 and $-0.846 \text{ e}/\text{\AA}^3$.

Results and Discussion

Syntheses and Characterizations. Three different clusters [$\text{Cu}_{11}(\mu_9\text{-Se})(\mu_3\text{-Br})_3\{\text{Se}_2\text{P}(\text{OR})_2\}_6$] (R = Et, Pr, ⁱPr) (**1a-c**) (43–47%), [$\text{Cu}_8(\mu_8\text{-Br})\{\text{Se}_2\text{P}(\text{OR})_2\}_6(\text{PF}_6)$] (**2a-c**) (13–17%), and [$\text{Cu}_8(\mu_8\text{-Se})\{\text{Se}_2\text{P}(\text{OR})_2\}_6$] (**3a-c**) (28–32%) were isolated (Scheme 1) from the reaction of $\text{Cu}(\text{CH}_3\text{CN})_4\text{PF}_6$, $\text{NH}_4\text{Se}_2\text{P}(\text{OR})_2$, and Bu_4NBr in a molar ratio of 2:3:2 in $\text{CH}_2\text{-Br}_2$ at 0 °C. However, when the reaction was carried out in a molar ratio of 4:3:1 (Cu/L/Br) under similar experimental condition, bromide-centered Cu_8 cube was the major product (48–58%) with small percentage (~19%) of selenium-centered cube and no Cu_{11} cluster was obtained (Scheme 2). This result was not unexpected as the chloride-centered Cu_8 cubes, [$\text{Cu}_8(\mu_8\text{-Cl})\{\text{Se}_2\text{P}(\text{OR})_2\}_6(\text{PF}_6)$],²³ were isolated in high yield with small amount of selenide-centered Cu_8 cube by using the molar ratio of 4:3:1 (Cu/L/Cl). Selenium-

centered Cu_8 cubes **3a-c** were reported earlier which formed without the presence of halide ion in solution.^{10,18,24}

The origin of the central selenium atom is probably from the diselenophosphate ligand. The formation of Se^{2-} from the ligand is not clear at this point; however, it is known that S^{2-} is from the oxidized ligand $\text{R}_2\text{P}(\text{S})\text{SS}(\text{S})\text{PR}_2$ for several Mo clusters.²⁵

The $^{31}\text{P}\{^1\text{H}\}$ NMR spectra of **1a-c** display a singlet at δ 81.7, 79.6, and 74.8 ppm accompanied by two sets of satellites (651 and 675 Hz for **1a**, 650 and 675 Hz for **1b**, and 647 and 668 Hz for **1c**) due to two inequivalent Se environments in the dsep ligands. ^{31}P and ^{77}Se NMR spectral data of **1a-2c** are given in Table 2. The observed inequivalence Se environments suggests a local C_{3h} symmetry is retained in solution (vide infra) as two Se environments cannot be interchanged by any symmetry operations of the C_{3h} point group. This is further supported by the observation of two sets of distinct chemical shift of the alkyl groups in the ^1H NMR spectrum. The $^{77}\text{Se}\{^1\text{H}\}$ NMR spectra of **1a-c** display two sets of resonance frequency (Figure 1a for **1a**) due to two chemically and magnetically inequivalent selenium nuclei, Se_A (connected to the 4-fold capped copper atom) and Se_B (connected to the 3-fold capped copper atom) of the dsep ligands (Figure 1b). Both Se_A and Se_B of the dsep ligands exhibit significantly different, intriguing scalar coupling patterns with adjacent chemically equivalent but magnetically nonequivalent phosphorus nuclei. The chemical shift centered at -5.7 , 9.2 , and 0.1 ppm are assigned due to Se_A and at 44.4 , 70.0 , and 61.7 ppm for Se_B in clusters **1a-c**, respectively. The largest couplings 677, 677, and 669 Hz (with Se_A) and 651, 651, and 650 Hz (with Se_B) in clusters **1a-c**, respectively, are due to the one-bond coupling to P_X to which the Se directly connected. These coupling constants are in good agreement with the ^{31}P NMR results. The remaining coupling pattern results from the three-bond coupling to the other two phosphorus nuclei. For Se_A the larger scalar coupling (34.5, 35.0, 34.8 Hz for **1a-c**, respectively) is due to the adjacent P_Y atom related to the 3-fold rotational axis and the torsion angles of $\text{Se}_A\text{-Cu-Se-P}_Y$ averaged 170.7° . The smaller one (14.4, 14.5, 14.7 Hz for **1a-c**, respectively) is due to the $\text{P}_{Z'}$ generated by the mirror plane having the averaged torsion angle of 162.8° . Surprisingly the coupling pattern of Se_B does not exhibit a similar pattern as that observed for Se_A . The three-bond coupling constant (9.0, 8.8, and 9.4 Hz for **1a-c**, respectively) is the result from the combination of coupling to two

(23) Liu, C. W.; Hung, C.-M.; Santra, B. K.; Chen, H.-C.; Hsueh, H.-H.; Wang, J.-C. *Inorg. Chem.* **2003**, *42*, 3216.

(24) Liu, C. W.; Hung, C.-M.; Wang, J.-C.; Keng, T.-C. *J. Chem. Soc., Dalton Trans.* **2002**, 3482.

(25) Haiduc, I.; Goh, L. Y. *Coord. Chem. Rev.* **2002**, *224*, 151.

Table 2. ^{31}P and ^{77}Se NMR Data for Compounds **1a–2c**^a

compd	$\text{Se}_2\text{P}(\text{OR})_2^-$, δ/ppm (J/Hz)	$\text{Se}_2\text{P}(\text{OR})_2^-$, δ/ppm (J/Hz)	Se^{2-} , δ/ppm
$[\text{Cu}_{11}(\mu_9\text{-Se})(\mu_3\text{-Br})_3\{\text{Se}_2\text{P}(\text{OEt})_2\}_6]$	81.7 ($^1J_{\text{P-SeB}} = 651$, $^1J_{\text{P-SeA}} = 675$)	44.4 ($^1J_{\text{BX}} = 651$, $^3J_{\text{BZ}} + ^3J_{\text{BY}} = 9.0$) −5.7 ($^1J_{\text{AX}} = 677$, $^3J_{\text{AY}} = 34.5$, $^3J_{\text{AZ}} = 14.4$)	−1220
$[\text{Cu}_{11}(\mu_9\text{-Se})(\mu_3\text{-Br})_3\{\text{Se}_2\text{P}(\text{OPr})_2\}_6]$	79.6 ($^1J_{\text{P-SeB}} = 650$, $^1J_{\text{P-SeA}} = 675$)	70.0 ($^1J_{\text{BX}} = 651$, $^3J_{\text{BZ}} + ^3J_{\text{BY}} = 8.8$) 9.2 ($^1J_{\text{AX}} = 677$, $^3J_{\text{AY}} = 35.0$, $^3J_{\text{AZ}} = 14.5$)	−1193
$[\text{Cu}_{11}(\mu_9\text{-Se})(\mu_3\text{-Br})_3\{\text{Se}_2\text{P}(\text{O}^i\text{Pr})_2\}_6]$	74.8 ($^1J_{\text{P-SeB}} = 647$, $^1J_{\text{P-SeA}} = 668$)	61.7 ($^1J_{\text{BX}} = 650$, $^3J_{\text{BZ}} + ^3J_{\text{BY}} = 9.4$) 0.1 ($^1J_{\text{AX}} = 669$, $^3J_{\text{AY}} = 34.8$, $^3J_{\text{AZ}} = 14.7$)	−1201
$[\text{Cu}_8(\mu_8\text{-Br})\{\text{Se}_2\text{P}(\text{OEt})_2\}_6](\text{PF}_6)$	74.2 (653)	−23.2 (650)	
$[\text{Cu}_8(\mu_8\text{-Br})\{\text{Se}_2\text{P}(\text{OPr})_2\}_6](\text{PF}_6)$	74.7 (652)	−16.7 (650)	
$[\text{Cu}_8(\mu_8\text{-Br})\{\text{Se}_2\text{P}(\text{O}^i\text{Pr})_2\}_6](\text{PF}_6)$	68.2 (648)	−0.2 (651)	

^a The symbols AX, AY, AZ, BX, BY, and BZ are according to Figure 1.

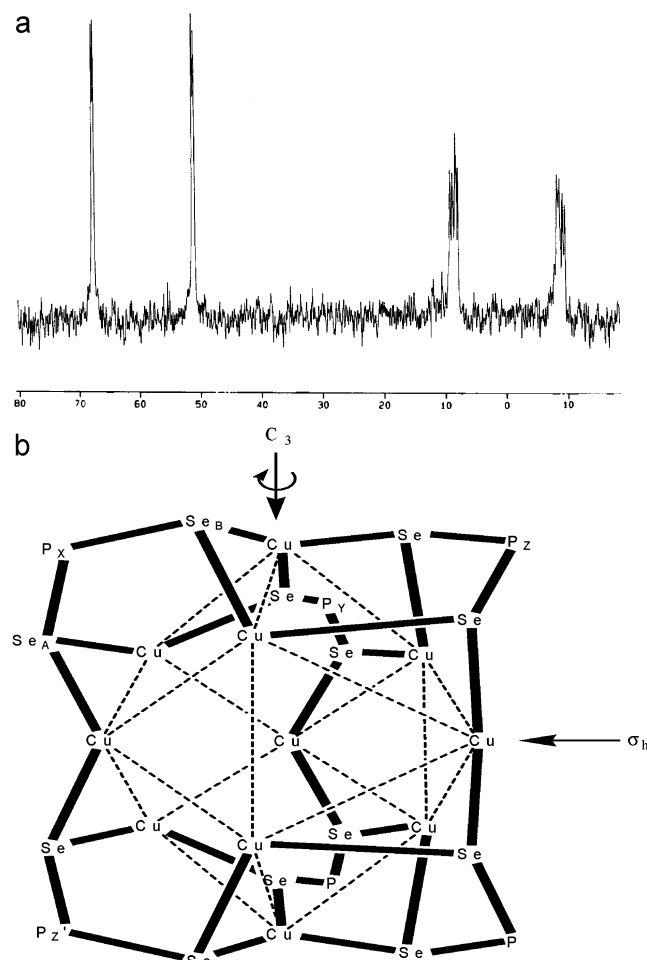


Figure 1. (a) $^{77}\text{Se}\{^1\text{H}\}$ NMR spectrum (CDCl_3) of $[\text{Cu}_{11}(\mu_9\text{-Se})(\mu_3\text{-Br})_3\{\text{Se}_2\text{P}(\text{OEt})_2\}_6]$. (b) $\text{Cu}_{11}\text{Se}_{12}\text{P}_6$ skeleton of cluster **1**.

adjacent P atoms (P_Y and P_Z) related to each other by the C_3 rotational axis. Presumably, these two $^3J(\text{Se}, \text{P})$ have opposite signs reflected in their averaged torsion angles of 176.2 and 18°, respectively. Due to the low natural abundance of ^{77}Se nuclei (<8%), it is unlikely that the coupling patterns mentioned above are from $^2J(\text{Se}, \text{Se})$ scalar coupling. The chemical shift for the central, noncoordinated selenium atom is at δ −1220, −1193, and −1201 ppm for **1a–c**, respectively. These data are close to the reported ones in $\text{Cu}_{11}(\mu_9\text{-Se})(\mu_3\text{-I})_3[\text{Se}_2\text{P}(\text{OR})_2]_6$.²⁴

In the positive FAB mass spectra of **1a–c**, in addition to the intact molecular peak, two major peaks which correspond to the loss of a bromide ion, $\{\text{Cu}_{11}(\mu_9\text{-Se})(\mu_3\text{-Br})_2[\text{Se}_2\text{P}$

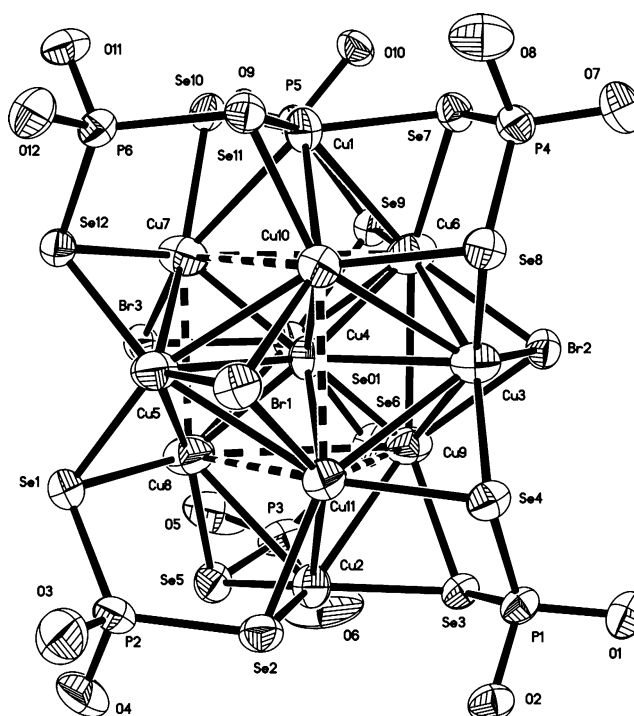


Figure 2. Thermal ellipsoid drawing (50% probability level) of $[\text{Cu}_{11}(\mu_9\text{-Se})(\mu_3\text{-Br})_3\{\text{Se}_2\text{P}(\text{O}^i\text{Pr})_2\}_6]$ with atom-numbering scheme. The isopropyl groups are omitted for clarity.

$(\text{OR})_2]_6\}^+$, and a dsep ligand, $\{\text{Cu}_{11}(\mu_9\text{-Se})(\mu_3\text{-Br})_3[\text{Se}_2\text{P}(\text{OR})_2]_5\}^+$, were identified.

$^{31}\text{P}\{^1\text{H}\}$ NMR spectra of **2a–c** display a singlet at δ 74.2, 74.7, and 68.2 ppm with satellites ($J_{\text{PSe}} = 653$, 652, and 648 Hz), respectively. The $^{77}\text{Se}\{^1\text{H}\}$ NMR spectra of **2a–c** show a doublet peak centered at −23.2, −16.7, and −0.2 ppm, respectively ($J_{\text{SeP}} = 650$ Hz for **1**, 650 Hz for **2**, and 651 Hz for **3**). Positive FAB mass spectra (FAB-MS) of **2a–c** in nitrobenzyl alcohol display the intact cationic cluster peaks.

Structure of $\text{Cu}_{11}(\mu_9\text{-Se})(\mu_3\text{-Br})_3[\text{Se}_2\text{P}(\text{O}^i\text{Pr})_2]_6$ (1c**).** In cluster **1c**, 11 copper atoms adopt the geometry of a 3,3,4,4,4-pentacapped trigonal prism with a selenium atom in the center (Figure 2). Selected bond lengths and angles are given in Table 3. A pseudo-3-fold axis passes through Cu1, Se01, and Cu2 atoms. A group of six copper atoms Cu7, Cu10, Cu6, Cu8, Cu11, and Cu9 form an idealized trigonal prism, of which each rectangular and triangular face is further capped by an additional copper atom. The edges of the trigonal prism are in the range of 3.431–3.590 Å while the heights (Cu7–Cu8, Cu10–Cu11, and Cu6–Cu9) are on

Table 3. Selected Bond Distances (Å) and Angles (deg) for **1c** with Esd's in the Parentheses

Cu(3)–Se(01)	2.748(2)	Cu(2)–Se(2)–Cu(11)	73.10(7)
Cu(4)–Se(01)	2.739(2)	Cu(1)–Se(10)–Cu(7)	72.54(7)
Cu(8)–Se(01)	2.580(2)	Cu(4)–Se(9)–Cu(6)	71.68(7)
Cu(11)–Se(01)	2.552(2)	Cu(5)–Se(12)–Cu(7)	73.34(7)
Cu(5)–Br(1)	2.452(2)	Se(4)–P(1)–Se(3)	117.88(13)
Cu(9)–Br(2)	2.622(2)	Se(2)–P(2)–Se(1)	119.1(2)
Cu(7)–Br(3)	2.539(2)	Se(8)–P(4)–Se(7)	118.16(14)
Cu(1)–Cu(10)	2.804(2)	P(6)–Se(12)–Cu(5)–Se(1)	163.91(10)
Cu(2)–Cu(8)	2.842(2)	P(3)–Se(5)–Cu(8)–Se(1)	165.03(12)
Cu(3)–Cu(9)	2.883(2)	P(3)–Se(5)–Cu(2)–Se(2)	177.50(11)
Cu(4)–Cu(7)	2.936(2)	P(1)–Se(3)–Cu(2)–Se(2)	14.96(12)
Cu(5)–Cu(11)	2.947(2)	P(3)–Se(5)–Cu(2)–Se(3)	22.30(14)
Cu(6)–Cu(9)	3.052(2)	P(2)–Se(2)–Cu(2)–Se(3)	179.54(11)
Cu(7)–Cu(10)	3.557(2)	P(4)–Se(8)–Cu(3)–Se(4)	163.46(10)
Cu(1)–Se(7)	2.378(2)	P(2)–Se(2)–Cu(11)–Se(4)	166.39(14)
Cu(2)–Se(2)	2.369(2)	P(1)–Se(3)–Cu(2)–Se(5)	175.24(11)
Cu(3)–Se(4)	2.436(2)	P(2)–Se(2)–Cu(2)–Se(5)	19.22(13)
Cu(4)–Se(9)	2.425(2)	P(5)–Se(9)–Cu(4)–Se(6)	164.05(10)
Cu(5)–Se(1)	2.430(2)	P(1)–Se(3)–Cu(9)–Se(6)	173.04(11)
Cu(9)–Se(3)	2.452(2)	P(5)–Se(10)–Cu(1)–Se(7)	16.85(12)
P–Se(av)	2.169(3)	P(6)–Se(11)–Cu(1)–Se(7)	175.33(10)
Se···Se(av)	3.731	P(1)–Se(4)–Cu(3)–Se(8)	164.71(10)
Cu(9)–Se(01)–Cu(10)	133.07(7)	P(6)–Se(11)–Cu(10)–Se(8)	173.94(11)
Cu(6)–Se(01)–Cu(7)	88.51(7)	P(3)–Se(6)–Cu(4)–Se(9)	157.47(11)
Cu(8)–Se(01)–Cu(4)	67.82(6)	P(4)–Se(7)–Cu(6)–Se(9)	173.10(11)
Cu(7)–Se(01)–Cu(3)	143.29(7)	P(4)–Se(7)–Cu(1)–Se(10)	174.66(10)
Cu(4)–Se(01)–Cu(3)	118.34(6)	P(6)–Se(11)–Cu(1)–Se(10)	17.67(12)
Cu(4)–Br(3)–Cu(7)	72.02(7)	P(5)–Se(10)–Cu(1)–Se(11)	175.17(10)
Cu(3)–Br(2)–Cu(9)	69.18(6)	P(4)–Se(7)–Cu(1)–Se(11)	17.00(12)
Cu(5)–Br(1)–Cu(11)	70.83(7)	P(2)–Se(1)–Cu(5)–Se(12)	163.18(12)
Cu(10)–Br(1)–Cu(11)	73.96(7)	P(5)–Se(10)–Cu(7)–Se(12)	172.68(10)

average 3.103 Å. Shorter Cu–Cu distances are observed between the capping atoms and the prism; they are in the range of 2.787–2.970 Å, comparable to the sum of the van der Waals radii for metallic copper (2.80 Å).²⁶ Alternatively the undecanuclear copper cage can be described as a combination of nine Cu₄ butterflies, where the wing-tip positions are represented by five capping copper atoms with each edge and height of the trigonal prism being the hinges. Clusters or cages having the geometry of pentacapped trigonal prism are not common; examples containing main-group elements as capping atoms are Ni₆(μ₃-Se)₂(μ₄-Se)₃-(PPh₃)₆²⁷ and [Cu₆(μ₃-I)₂(μ₄-I)₃I₆].^{5–28} The undecanuclear silver clusters containing diethyl dithiocarbamate ligands of the type Ag₁₁(μ₅-E)(μ₄-Et₂NCS₂)₃(μ₃-Et₂NCS₂)₆ (E = S²⁻, Se²⁻)²⁹ are known where central S²⁻ or Se²⁻ is connected to five silver atoms in a trigonal bipyramidal geometry. The iodo analogues of **1** were reported from this group.²⁴

For the capping Cu atoms (Cu3, Cu4, Cu5) the Cu–μ₉-Se01 bond distances are slightly longer, 2.736–2.748 Å (within reported limits),³⁰ compared to those Cu atoms in the trigonal prism which are between 2.519 and 2.580 Å. The Cu–Se01–Cu angles are in the range of 65.12–144.15°.

(26) Bondi, A. *J. Phys. Chem.* **1964**, *68*, 441.

(27) Fenske, D.; Ohmer, J. *Angew. Chem., Int. Ed. Engl.* **1987**, *26*, 148.

(28) Mahdjour-Hassen-Abadi, F.; Harts, H.; Fuchs, J. *Angew. Chem., Int. Ed. Engl.* **1984**, *23*, 514.

(29) (a) Zhang, Q.-F.; Cao, R.; Hong, M.-C.; Su, W.-P.; Liu, H.-Q. *Inorg. Chim. Acta* **1998**, *277*, 171. (b) Huang, Z. Y.; Lei, X. J.; Hong, M. C.; Liu, H. Q. *Inorg. Chem.* **1992**, *31*, 2991. (c) Su, W. P.; Hong, M. C.; Jiang, F. L.; Liu, H. Q.; Zhou, Z. Y.; Wu, D. D.; Mak, T. C. W. *Polyhedron* **1996**, *15*, 4047.

(30) (a) Zhu, N.-Y.; Fenske, D. *J. Chem. Soc., Dalton Trans.* **1999**, 1067. (b) Semmelmann, M.; Fenske, D.; Corrigan, J. F. *J. Chem. Soc., Dalton Trans.* **1998**, 2541. (c) Deveson, A.; Dehnen, S.; Fenske, D. *J. Chem. Soc., Dalton Trans.* **1997**, 4491.

The central core is further stabilized by three bromides and six dsep ligands. The Cu₄ butterflies containing a copper atom on the C₃ axis are each capped by a dsep ligand having a tetrametallic tetraconnective (μ₂, μ₂) coordination pattern.³¹ The Cu–μ₂-Se distances lie in the range between 2.350 and 2.502 Å, and the Cu–μ₂-Se–Cu angles range between 70.61 and 73.73°. The P–Se distances average 2.168 Å. The Se···Se “bite” distances average 3.731 Å and are slightly shorter than those (3.776 and 3.784 Å) found in the Cu₈ cube.^{10,24} This is as expected when taking into account the difference in the capping faces: butterfly and square. The remaining three, where hinge positions are the heights of the prism, are each capped by a triply bridging bromide atom over an alternating set of three of the six triangular faces. The average Cu–Br bond distance is 2.541 Å. The Cu–Br–Cu angles are in the range 69.18 and 73.96°. Overall, due to the existence of three alternating triply bridging bromides, the idealized D_{3h} symmetry of the Cu₁₁Se unit is lowered to C_{3h}. Hence, all the dsep ligands are related to each other by the virtual 3/m symmetry.

Structure of [Cu₈(μ₈-Br){Se₂P(OR)₂}]₆ (PF₆) [R = Et (2a), iPr (2c)]. The crystal structures of **2a,c** consist of a cationic cluster in which eight copper ions are linked by six diselenophosphate ligands with a central μ₈-Br ion. The shape of the molecule is a bromide-centered distorted Cu₈ cube where the copper atoms are arranged at the corner of the cube. Each selenium atom of the dsep ligand bridges two copper atoms. Thus dsep ligand exhibits a tetrametallic tetraconnective (μ₂, μ₂) coordination pattern³¹ and each occupies a square face of the cube. Each copper atom of the cube is coordinated by three selenium atoms of three different ligands. In addition to the trigonal planar geometry around the copper atom, there is a strong interaction to the central bromide ion.

The compound **2a** is crystallized with solvated H₂O molecules in the trigonal space group R $\bar{3}c$, whereas compound **2c** crystallizes in the monoclinic space group C2/c. Selected bond lengths and angles are given in Table 4. Due to the absence of inversion center in **2a**, the Br(1) atom does not locate exactly in the center of the cube (Figure 3). In **2c**, four copper atoms are found in the asymmetric unit with the Br atom located in the center of inversion. The Cu–Br distances span in the range 2.695–2.797 Å for **2a** and 2.733–2.771 Å for **2c**. The averaged Cu–Cu distances are 3.192 and 3.176 Å for **2a,c**, respectively, slightly longer than Cu–Cu distance, 3.14 Å, in chloride-centered Cu₈ cubes.²³ The Cu–Se bond distances lie in the range 2.360–2.404 and 2.374–2.399 Å, respectively, comparable to 2.365–2.408 Å in chloride-centered Cu₈ cubes. The averaged P–Se distances are 2.17 and 2.169 Å, respectively. The averaged Se···Se bite distances are 3.807 and 3.823 Å, respectively, longer than 3.784 Å in selenium-centered cubes.¹⁰ The Se–Cu–Se angle ranges from 116.22 to 121.30° and 117.18 to 120.24°, respectively. The Cu–Br–Cu angles lie in the range

(31) Haiduc, I.; Sowerby, D. B.; Lu, S.-F. *Polyhedron* **1995**, *14*, 3389.

Table 4. Selected Bond Distances (Å) and Angels (deg) for **2a**·3/2H₂O and **2c** with Esd's in Parentheses

2a		2c	
Br(1)–Cu(1)	2.774(2)	Br–Cu(1)	2.756(1)
Br(1)–Cu(2)	2.698(2)	Br–Cu(2)	2.757(1)
Br(1)–Cu(3)	2.761(3)	Br–Cu(3)	2.771(1)
Br(1)–Cu(4)	2.792(3)	Br–Cu(4)	2.733(1)
Cu(1)–Se(1)	2.389(2)	Cu(1)–Se(2)	2.374(1)
Cu(1)–Se(3)	2.370(2)	Cu(1)–Se(6)	2.382(1)
Cu(1)–Se(4B)	2.392(2)	Cu(1)–Se(1A)	2.382(2)
Cu(2)–Se(2)	2.404(2)	Cu(2)–Se(5)	2.392(1)
Cu(2)–Se(3)	2.393(2)	Cu(2)–Se(6)	2.391(1)
Cu(2)–Se(4)	2.400(2)	Cu(2)–Se(3A)	2.395(1)
Cu(3)–Se(2)	2.360(2)	Cu(3)–Se(1)	2.395(1)
Cu(4)–Se(1)	2.393(1)	Cu(4)–Se(2)	2.396(1)
P–Se(av)	2.168(4)	P–Se(av)	2.177(2)
Se····Se(av)	3.807	Se····Se(av)	3.823
Se–P–Se(av)	122.64(15)	Se–P–Se(av)	122.71(10)
Cu(2)–Br(1)–Cu(3)	69.85(5)	Cu(2)–Br–Cu(3)	69.40(3)
Cu(2A)–Br(1)–Cu(1B)	72.06(5)	Cu(2A)–Br–Cu(1A)	70.98(4)
Cu(2B)–Br(1)–Cu(1B)	68.28(5)	Cu(2A)–Br–Cu(4)	71.97(3)
Cu(1)–Br(1)–Cu(4)	71.94(5)	Cu(3)–Br–Cu(4)	70.60(3)
Cu(1)–Se(1)–Cu(4)	86.28(8)	Cu(1)–Se(2)–Cu(4)	82.32(5)
Cu(3)–Se(2)–Cu(2)	81.99(9)	Cu(3)–Se(5)–Cu(2)	82.29(5)
Cu(1)–Se(3)–Cu(2)	80.31(7)	Cu(1)–Se(6)–Cu(2)	84.20(5)
Cu(1A)–Se(4)–Cu(2)	84.38(7)	Cu(4)–Se(4)–Cu(3)	83.12(4)
Se(3)–Cu(1)–Se(1)	121.30(8)	Se(3)–Cu(4)–Se(2)	117.18(5)
Se(3)–Cu(1)–Se(4B)	118.45(8)	Se(3)–Cu(4)–Se(4)	118.18(5)
Se(1)–Cu(1)–Se(4B)	116.84(7)	Se(2)–Cu(4)–Se(4)	120.24(5)
Se(3)–Cu(1)–Br(1)	98.64(7)	Se(3)–Cu(4)–Br	95.70(4)
Se(1)–Cu(1)–Br(1)	95.36(7)	Se(1)–Cu(3)–Br	96.04(4)
Cu(1)–Se(1)–P(1)	107.00(11)	Cu(1)–Se(2)–P(2)	103.83(8)
Cu(4)–Se(1)–P(1)	97.22(10)	Cu(4)–Se(2)–P(2)	104.49(7)

68.28–72.06° for **2a** and 69.40–71.97° for **2c** where as in the perfect cube this angle is 70.53°. ³²

DFT Calculations. Molecular orbital calculations at the B3LYP level of theory have been carried out to study the Cu– μ_9 -Se interactions for clusters Cu₁₁(μ_9 -Se)(μ_3 -X)₃{Se₂P(OR)₂}₆ (X = Br, I). ³³ Similar to our early study on the cubic clusters Cu₈(μ_8 -Se)[Se₂P(OR)₂]₆, ³⁴ the molecular orbital calculations show that the three p orbitals of the central Se atom make the major contribution to the highest occupied molecular orbitals (HOMOs), indicating that the interactions between the μ_9 -Se atom and the Cu metal atoms in the cluster

framework are weak. The weak interactions do not provide sufficient stabilization energies to the orbitals constituted mainly from the central Se atom. Therefore, these occupied orbitals have the highest orbital energies and are the HOMOs. The LUMOs in the clusters correspond to those orbitals having the P–Se σ^* antibonding characters.

In the early study ³⁴ on Cu₈(μ_8 -Se){Se₂P(OR)₂}₆, a bond order of 1/2, with respect to a normal Cu–Se bond between Cu and Se from the Se₂P(OR)₂ ligands, was formally suggested to the description of the Cu– μ_8 -Se bonding interaction. The formal bond order assignment was based on the consideration that there are only four occupied bonding molecular orbitals, which represent the valence shell of the central Se atom, responsible for the bonding interactions between the eight copper atoms and the central atom.

The two clusters, Cu₁₁(μ_9 -Se)(μ_3 -X)₃{Se₂P(OR)₂}₆ (X = Br, I), studied here are isostructural. In each cluster, the Cu₁₁ metal framework can be described as pentacapped trigonal prismatic (TP). Among the 11 Cu atoms, there are only 9 Cu atoms having bonding interactions with the central Se atom because 2 Cu atoms cap the 2 triangle faces of the TP structure and are too far away from the central μ_9 -Se atom. Now, one has a situation as follows. The four bonding molecular orbitals that represent the valence shell of the central atoms are shared among nine Cu– μ_9 -Se bonds. It is therefore expected that the formal bond order of each Cu– μ_9 -Se bond should be slightly smaller than 1/2. Indeed, the natural bond order (NBO) analyses ³⁵ (Table 5) from the molecular orbital calculations show that the Wiberg bond indices (measure of bond strength) ³⁶ calculated for Cu– μ_9 -Se are either approximately half or smaller than half of those calculated for the terminal Cu–Se bonds. The 11 Cu atoms can be categorized into three types (Figure 4). Cu¹ represents the type of atoms occupying the six corners of the trigonal prism (TP). Cu² represents the type of atoms capping the three square faces of the TP. Cu³ represents the type of atoms capping the two triangular faces of the TP.

A smaller formal bond order suggested for each of the Cu– μ_9 -Se bonds in the two clusters studied here is also consistent with the experimental observations. The Cu– μ_9 -Se bond distances in Cu₁₁(μ_9 -Se)(μ_3 -X)₃{Se₂P(OR)₂}₆ (X = Br, I) are generally longer than the corresponding Cu– μ_8 -Se bond distances in Cu₈(μ_8 -Se){Se₂P(OR)₂}₆. The average Cu¹– μ_9 -Se and Cu²– μ_9 -Se bond distances are 2.56 and 2.74 Å, respectively, in Cu₁₁(μ_9 -Se)(μ_3 -Br)₃{Se₂P(OR)₂}₆ and are 2.61 and 2.69 Å, respectively, in Cu₁₁(μ_9 -Se)(μ_3 -I)₃{Se₂P(OR)₂}₆. The average Cu– μ_8 -Se bond distance in Cu₈(μ_8 -Se){Se₂P(OR)₂}₆ is ca. 2.52 Å, shorter than those mentioned above.

As mentioned above, the two clusters studied here are isostructural. It is interesting to note that the average Cu¹– μ_9 -Se bond distance in Cu₁₁(μ_9 -Se)(μ_3 -Br)₃{Se₂P(OR)₂}₆ is shorter than that in Cu₁₁(μ_9 -Se)(μ_3 -I)₃{Se₂P(OR)₂}₆. However, the situation for the average Cu²– μ_9 -Se bond distances is

(32) Schugar, H. J.; Ou, C.-C.; Thich, J. A.; Lalancette, R. A.; Furey, W., Jr. *J. Am. Chem. Soc.* **1976**, *98*, 3047.

(33) Density functional calculations at the B3LYP level were performed on the model clusters Cu₁₁(μ_9 -Se)(μ_3 -X)₃{Se₂P(OH)₂}₆ (X = Br, I) based on the experimentally determined structures of Cu₁₁(μ_9 -Se)(μ_3 -X)₃{Se₂P(OⁱPr)₂}₆ (X = Br, I). The basis set used for O and H atoms was 6-31G, while an effective core potential with a LanL2DZ basis set was employed for Cu, P, and Se. The DFT calculations were performed with the use of the Gaussian 98 package: Frisch, M. J.; Trucks, G. W.; Schlegel, H. B.; Scuseria, G. E.; Robb, M. A.; Cheeseman, J. R.; Zakrzewski, V. G.; Montgomery, J. A. Jr.; Stratmann, R. E.; Burant, J. C.; Dapprich, S.; Millam, J. M.; Daniels, A. D.; Kudin, K. N.; Strain, M. C.; Farkas, O.; Tomasi, J.; Barone, V.; Cossi, M.; Cammi, R.; Mennucci, B.; Pomelli, C.; Adamo, C.; Clifford, S.; Ochterski, J.; Petersson, G. A.; Ayala, P. Y.; Cui, Q.; Morokuma, K.; Malick, D. K.; Rabuck, A. D.; Raghavachari, K.; Foresman, J. B.; Cioslowski, J.; Ortiz, J. V.; Stefanov, B. B.; Liu, G.; Liashenko, A.; Piskorz, P.; Komaromi, I.; Gomperts, R.; Martin, R. L.; Fox, D. J.; Keith, T.; Al-Laham, M. A.; Peng, C. Y.; Nanayakkara, A.; Gonzalez, C.; Challacombe, M.; Gill, P. M. W.; Johnson, B.; Chen, W.; Wong, M. W.; Andres, J. L.; Gonzalez, C.; Head-Gordon, M.; Replogle, E. S.; Pople, J. A. *GAUSSIAN98*, revision A.9; Gaussian, Inc.: Pittsburgh, PA, 1998.

(34) Liu, C. W.; Hung, C.-M.; Santra, B. K.; Wang, J.-C.; Hsien-Ming Kao, H.-M.; Lin, Z. *Inorg. Chem.* **2003**, *42*, 8551.

(35) Reed, A.; Curtiss, L. A.; Weinhold, F. *Chem. Rev.* **1988**, *88*, 899.

(36) Wiberg, K. B. *Tetrahedron* **1968**, *24*, 1083. The Wiberg bond indices (bond orders) are a measure of bond strength.

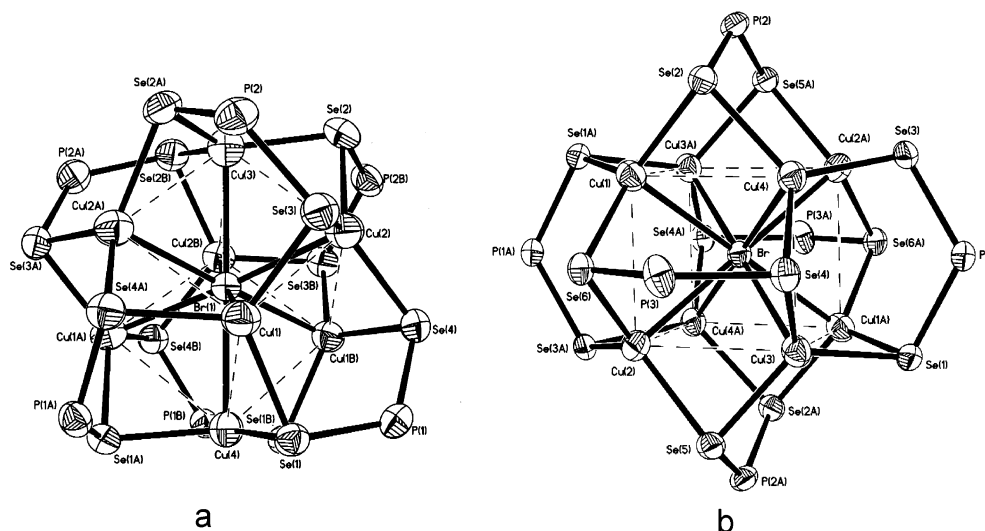


Figure 3. Thermal ellipsoid drawings (50% probability level) of the cation of clusters, $\text{Cu}_8(\mu_8\text{-Br})[\text{Se}_2\text{P}(\text{OEt})_2]_6(\text{PF}_6) \cdot 3/2\text{H}_2\text{O}$ (a) and $\text{Cu}_8(\mu_8\text{-Br})[\text{Se}_2\text{P}(\text{O}^i\text{Pr})_2]_6(\text{PF}_6)$ (b), showing atom-numbering schemes. The alkoxyl groups are omitted for clarity.

Table 5. Results of Natural Bond Order and Population Analyses Together with the HOMO–LUMO Gaps Calculated for $\text{Cu}_{11}(\mu_9\text{-Se})(\mu_3\text{-X})_3\{\text{Se}_2\text{P}(\text{OPR}^i)_2\}_6$ (X = Br, I)^a

param	atom(s)	cluster	
		$\text{Cu}_{11}(\mu_9\text{-Se})(\mu_3\text{-Br})_3\{\text{Se}_2\text{P}(\text{OPR}^i)_2\}_6^b$	$\text{Cu}_{11}(\mu_9\text{-Se})(\mu_3\text{-I})_3\{\text{Se}_2\text{P}(\text{OPR}^i)_2\}_6^b$
Wiberg bond index	$\text{Cu}^1\text{-}\mu_9\text{-Se}$	0.10	0.09
	$\text{Cu}^2\text{-}\mu_9\text{-Se}$	0.06	0.07
	$\text{Cu}^3\text{-}\mu_9\text{-Se}$	0.02	0.02
	$\text{Cu}^1\text{-}\mu_3\text{-X}$	0.13	0.17
	$\text{Cu}^2\text{-}\mu_3\text{-X}$	0.20	0.23
	$\text{Cu}\text{-Se}(\text{terminal})$	0.20	0.19
natural charge	Cu^1	0.62	0.60
	Cu^2	0.62	0.60
	Cu^3	0.59	0.59
	$\mu_9\text{-Se}$	-1.41	-1.41
	$\mu_3\text{-X}$	-0.67	-0.59
HOMO–LUMO gap	$\text{Se}(\text{terminal})$	-0.55	-0.55
		3.56 eV	3.49 eV

^a The Cu_{11} metal framework in each cluster can be described as pentacapped trigonal prismatic. Therefore, there are three types of Cu atoms. Cu^1 represents the type of atoms occupying the six corners of the trigonal prism (TP). Cu^2 represents the type of atoms capping the three square faces of the TP. Cu^3 represents the type of atoms capping the two triangular faces of the TP. ^b The alkyl groups were replaced with hydrogen atoms in the model calculations.

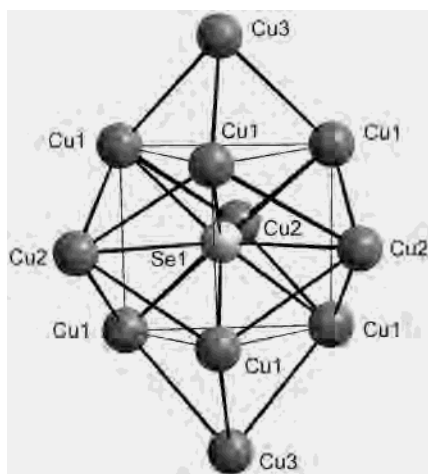


Figure 4. Eleven Cu atoms categorized into three types, Cu^1 , Cu^2 , and Cu^3 , representing the Cu atoms occupying the six corners of the trigonal prism (TP), capping the three square-faces, and capping the two triangular faces of the TP, respectively.

the opposite. The average $\text{Cu}^2\text{-}\mu_9\text{-Se}$ bond distance in $\text{Cu}_{11}\text{-}(\mu_9\text{-Se})(\mu_3\text{-Br})_3[\text{Se}_2\text{P}(\text{OR})_2]_6$ is longer than that in $\text{Cu}_{11}\text{-}(\mu_9\text{-Se})(\mu_3\text{-I})_3[\text{Se}_2\text{P}(\text{OR})_2]_6$.

$\text{Se})(\mu_3\text{-I})_3[\text{Se}_2\text{P}(\text{OR})_2]_6$. With careful examination of the structural details of the two clusters, we come to the following plausible explanation. Due to the significantly larger size of I^- in comparison to Br^- , the repulsion interactions between the $\mu_3\text{-I}$ ligands and Se from the terminal $[\text{Se}_2\text{P}(\text{OR})_2]$ ligands are expected to be greater. To make effective $\text{Cu}^1\text{-}\mu_3\text{-I}$ bonding and minimize the ligand repulsion, the six Cu^1 atoms move away slightly from the central Se atom. At the same time, the three Cu^2 atoms, which are intrinsically farther away from the central Se atom, move closer to the center to balance the $\text{Cu}\text{-}\mu_9\text{-Se}$ interactions. The weak $\text{Cu}\text{-}\mu_9\text{-Se}$ interactions make it possible that one set of Cu's moves in and the other moves out.

The different halide ligands do not cause much difference in the natural atomic charges calculated for the copper atoms between the two clusters (Table 5). Therefore, the charge argument, which was proposed previously³⁴ to explain the metal core contraction from $\text{Cu}_8(\mu_8\text{-Se})\{\text{S}_2\text{P}(\text{OR})_2\}_6$ to $\text{Cu}_8(\mu_8\text{-Se})\{\text{Se}_2\text{P}(\text{OR})_2\}_6$, is not applicable here. The change in the natural atomic charges of Cu from $\text{Cu}_8(\mu_8\text{-Se})\{\text{S}_2\text{P}(\text{OR})_2\}_6$ to $\text{Cu}_8(\mu_8\text{-Se})[\text{Se}_2\text{P}(\text{OR})_2]_6$ is more significant be-

cause there are 12 chalcogenide ligands involved. In the two clusters studied here, the difference involves only three halide ligands. It would be an interesting comparison if we could obtain $\text{Cu}_{11}(\mu_9\text{-Se})(\mu_3\text{-X})_3[\text{S}_2\text{P}(\text{OR})_2]_6$ in the future.

The HOMO–LUMO gaps of the two clusters are close to each other (Table 5). The slightly smaller gap calculated for $\text{Cu}_{11}(\mu_9\text{-Se})(\mu_3\text{-I})_3\{\text{Se}_2\text{P}(\text{OR})_2\}_6$ is consistent with the fact that I^- is more electron-donating than Br^- and pushes up the HOMOs in energy.

Conclusion

Undecanuclear copper clusters, $[\text{Cu}_{11}(\mu_9\text{-Se})(\mu_3\text{-Br})_3\{\text{Se}_2\text{P}(\text{OR})_2\}_6]$ ($\text{R} = \text{Et}, \text{Pr}, \text{iPr}$), possessing a 3,3,4,4,4-pentacapped trigonal prismatic copper framework, were isolated along with the bromide- and selenide-centered Cu_8 cubic clusters. The central core, Cu_{11}Se , having a nonacoordinated selenium atom in a tricapped trigonal prismatic geometry, was further stabilized by three bromides and six dsep ligands. ^{77}Se NMR

spectra of these clusters are of special interest because two inequivalent selenium nuclei of the diselenophosphate ligand exhibit different scalar coupling patterns with the adjacent phosphorus nuclei which are reminiscent of their averaged torsion angles of $\text{Se}-\text{Cu}-\text{Se}-\text{P}$. Molecular orbital calculations at the B3LYP level of the density functional theory have shown that the formal bond order of each $\text{Cu}-\mu_9\text{-Se}$ bond is slightly smaller than half of those calculated for the terminal $\text{Cu}-\mu_2\text{-Se}$ bonds revealed in undecanuclear copper clusters, $\text{Cu}_{11}(\mu_9\text{-Se})(\mu_3\text{-X})_3\{\text{Se}_2\text{P}(\text{OR})_2\}_6$ ($\text{X} = \text{Br}, \text{I}$).

Acknowledgment. We thank the National Science Council of Taiwan (Grant NSC 92-2113-M-033-012) for the financial support.

Supporting Information Available: X-ray crystallographic files in CIF format for the compound **2a**. This material is available free of charge via the Internet at <http://pubs.acs.org>.

IC049589J